Inorganic Chemistry

Article

pubs.acs.org/IC

$[(Pb_6I_8)\{Mn(CO)_5\}_6]^{2-}$: An Octahedral (M_6X_8)-like Cluster with Inverted Bonding

Silke Wolf,[†] Kevin Reiter,[‡] Florian Weigend,[‡,§] Wim Klopper,[‡,§] and Claus Feldmann*[,†]

[†]Institut für Anorganische Chemie, Karlsruhe Institute of Technology (KIT), Engesserstrasse 15, D-76131 Karlsruhe, Germany

[‡]Institut für Physikalische Chemie, Karlsruhe Institute of Technology (KIT), Fritz-Haber-Weg 2, D-76131 Karlsruhe, Germany

[§]Institut für Nanotechnologie, Karlsruher Institut für Technologie (KIT), Hermann-von-Helmholtz-Platz 1, D-76344 Eggenstein-Leopoldshafen, Germany

ABSTRACT: $[BMIm]_2[\{PbMn(CO)_5\}_6I_8]$ (BMIm: 1-butyl-3-methylimidazolium) is obtained by ionic liquid mediated reaction of PbI_2 and $Mn_2(CO)_{10}$. Central is a cubelike (Pb_6I_8) unit containing a nonfilled Pb_6 octahedron. Each Pb of this (Pb_6I_8) unit is terminated on its outside by $Mn(CO)_5$, exhibiting Pb−Mn metal-to-metal bonding (280 pm). Structurally, the (Pb_6I_8) unit is similar to the well-known octahedral (M_6X_n) cluster-type family (M = Zr, Nb, Ta, Mo, W; X = Cl, Br, I). In contrast to most similar cluster compounds, such as W_6Br_{12} ($[W_6Br_8]Br_{2/1}Br_{4/2}$, according to Niggli notation) or the carbonyl cluster $[Sn_6\{Cr(CO_5)_6\}]^{2-}$, however, the nonfilled central Pb_6 octahedron in $[\{PbMn(CO)_5\}_6I_8]^{2-}$ does not exhibit any metal-to-metal bonding. Structure and bonding of the title compound are validated by single-crystal structure analysis, energy-dispersive X-ray analysis (EDX), infrared spectroscopy (FT-IR), and density functional theory (DFT) calculations. Based on the isolobal principle, electronegativity considerations, bond lengths, and DFT calculations including Mulliken population analysis and natural population analysis (NPA), in sum, the charge distribution of Pb is best reflected by an oxidation state of +1.

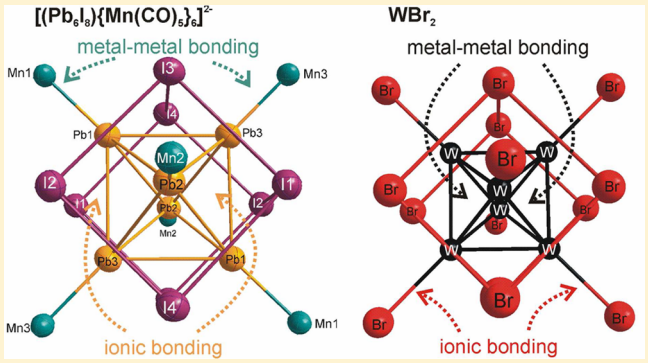

INTRODUCTION

Octahedral metal clusters (M_6X_n) (n = 8−18) are well-known for a wide range of transition-metal halogenides and chalcogenides.[1] Prominent examples include the compounds M_6X_{12}/M_6X_{18} (M = Mo, W; X = Cl, Br, I),[2] M_6X_{12} (M = Zr, Nb, Ta; X = Cl, Br, I),[3] MNb_8O_{14} (M = metal),[4] or the Chevrel phases $M_xM'_6Y_8$ (with M = metal; M′ = Mo, Re; Y = S, Se, Te).[5] Metal−metal interactions of the respective central $(M^{2+}/M^{3+})_6$ octahedron are characteristic for all these compounds and essential for their existence. The cluster backbone is predominantly established by metal-*d*-orbitals.[1,6] Often these transition-metal clusters have a high chemical and physical stability; in part, the molecular clusters even exist in solution.[1]

In contrast to the manifold of octahedral transition-metal clusters, similar $(M^{2+}/M^{3+})_6$ clusters have not yet been identified for main-group metals. A comparable structural motif was observed in the Zintl-like carbonyl cluster $[Sn_6\{Cr(CO_5)_6\}]^{2-}$ that is essentially established by metal-to-metal bonding of the central Sn_6 octahedron as well.[7] Being right comparable to the Zintl ion $[Sn_6]^{2-}$, the oxidation state of tin in $[Sn_6\{Cr(CO_5)_6\}]^{2-}$ is <0 and, therefore, also different from the above-mentioned octahedral (M_6X_n) transition-metal clusters. Although expected as less stable,[8] the existence of octahedral $(M^{2+/3+})_6$ main-group-metal clusters has been predicted nevertheless by density-functional theory (DFT) calculations.[9] For Pb_6, for instance, the global minimum structure was reported to be a (flattened) octahedron.

In the following, we report on $[BMIm]_2[(Pb_6I_8)\{Mn(CO)_5\}_6]$ (BMIm: 1-butyl-3-methylimidazolium) containing the carbonyl cluster anion $[(Pb_6I_8)\{Mn(CO)_5\}_6]^{2-}$. The compound was prepared by reaction of $Mn_2(CO)_{10}$ and PbI_2 in the ionic liquid $[BMIm][NTf_2]$ (BMIm, 1-butyl-3-methylimidazolium; NTf_2, bis-trifuoromethansulfonimide). Since $\{Mn(CO)_5\}^-$ is isolobal to a halogenide anion X^-,[10] the similarity between $[(Pb_6I_8)\{Mn(CO)_5\}_6]^{2-}$ and (M_6X_8) transition-metal clusters (M = Zr, Nb, Ta, Mo, W; X = Cl, Br, I) is even more obvious.[2] However, the title compound shows inverted bonding with Pb−Mn metal-to-metal bonding on the outside, but not any Pb−Pb metal−metal bonding of the central Pb_6 octahedron.

EXPERIMENTAL METHODS

Chemicals. All compounds and sample handling was carried out under argon, applying standard Schlenk and glovebox techniques. The reaction took place in argon-filled and sealed glass ampules, which were dried under reduced pressure (10^{-3} mbar) at 300 °C before use. The commercially available starting materials $Mn_2(CO)_{10}$ (98%, Sigma−Aldrich) and PbI_2 (99.99%, ABCR) were used as supplied. The ionic liquid $[BMIm][NTf_2]$ (BMIm, 1-butyl-3-methylimidazo-

Received: January 23, 2015
Published: April 1, 2015

DOI: 10.1021/acs.inorgchem.5b00170
Inorg. Chem. 2015, 54, 3989−3994

lium; NTf_2, bis-trifuoromethansulfonimide) was synthesized via metathesis from Li(NTf_2) (99%, 3M) and 1-butyl-3-methylimidazolium chloride (99%, Iolitec) in water. The resulting ionic liquid was extracted with methylene chloride, washed with deionized water, and finally dried under reduced pressure (10^{-3} mbar) at 80 °C for 48 h.

Synthesis of $[BMIm]_2[(Pb_6I_8)\{Mn(CO)_5\}_6]$. PbI_2 (100 mg, 0.4 mmol) and $Mn_2(CO)_{10}$ (78.6 mg, 0.2 mmol) were dissolved in the ionic liquid [BMIm][NTf_2]. This solution was sealed in a glass ampule and heated at 130 °C for 20 days. After cooling to room temperature with a rate of 1 K h^{-1}, red crystals of the title compound were obtained. The crystals were separated from the ionic liquid by filtration through a glass filter and washed with the pure ionic liquid to remove nonreacted starting materials. Subsequent to washing and removal of the ionic liquid, the title compound was obtained with a yield of ~20%. The synthesis of larger quantities is restricted by three aspects:

(i) The solubility of the ionic liquid and the title compound are very similar, since the $[BMIm]^+$ cation of the ionic liquid is incorporated in both compounds. Washing, for example, with cooled diethyl ether to remove the ionic liquid results in partial dissolution of the $[BMIm]_2[(Pb_6I_8)\{Mn(CO)_5\}_6]$ crystals as well.

(ii) Washing with diethyl ether, moreover, leads to a precipitation of MnI_2, thereafter sticking on the surface of the $[BMIm]_2[(Pb_6I_8)\{Mn(CO)_5\}_6]$ crystals.

(iii) Finally, $[BMIm]_2[(Pb_6I_8)\{Mn(CO)_5\}_6]$ slowly decomposes, even at room temperature, under a release of CO.

Data Collection. Data collection of $[BMIm]_2[(Pb_6I_8)\{Mn(CO)_5\}_6]$ was performed at 200 K on an IPDS II image plate diffractometer (Stoe, Darmstadt, Germany), using graphite-monochromatized Mo Kα (71.073 pm) radiation and a low-temperature device. For measurement, suitable crystals were isolated in inert oil and mounted on a glass capillary. After data reduction by X-RED (Stoe, Data Reduction Program, Version 1.14, Darmstadt, Germany, 1999), space-group determination was carried out on the basis of symmetry equivalences and systematic absences by XPREP (Stoe, Data Reduction Program, Version 1.14, Darmstadt, Germany, 1999). Structure solution and refinement were performed by direct methods and refined by full-matrix least-squares against F^2 with SHELXTL (Bruker, Structure Solution and Refinement Package, Version 5.1, Karlsruhe, Germany, 1998). The results are listed in Table 1. All non-hydrogen atoms were refined with anisotropic displacement parameters. The position of the hydrogen atoms could not be fixed by Fourier refinement and was therefore modeled based on idealized C−H bonds. X-SHAPE (Stoe, Crystal Optimisation for Numerical Absorption Correction, Version 1.06, Darmstadt, Germany, 1999) was used to apply a numerical absorption correction, based on crystal-shape optimization. Note that the highest residual electron density was observed in the central Pb_6 octahedron in close distance to each lead atom (<1 Å). This finding can be related to the lone pairs at each of the lead atoms (cf. Figure 4b, presented later in this work). Illustrations of the crystal structures were prepared via DIAMOND (Crystal Impact, Visuelles Informationssystem für Kristallstrukturen, Version 3.0d, Bonn, Germany, 2005). CCDC 1001803 contains the supplementary crystallographic data for this paper. These data can be obtained free of charge from the Cambridge Crystallographic Data Centre (CCDC) via www.ccdc.cam.ac.uk/data_request/cif.

Energy-Dispersive X-ray (EDX) Analysis. EDX was carried out using an AMETEC EDAX mounted on a Zeiss SEM Supra 35 VP scanning electron microscope. For measurement, single crystals were fixed with conductive carbon pads on aluminum sample holders.

Fourier Transform Infrared (FT-IR) Spectroscopy. The infrared spectrum was recorded on a Bruker Vertex 70 FT-IR spectrometer (Bruker); the sample was measured as a pellet in KBr. For this purpose, 300 mg of dried KBr and 2 mg of the sample were carefully ground together with a mortar and pestle and pressed to a thin pellet.

Optimized Geometry of $[(Pb_6I_8)\{Mn(CO)_5\}_6]^{2-}$. All calculations were performed with the TURBOMOLE program package.[11] The TPSS functional[12] was used with the dhf-TZVP basis[13] and grid m4 for numerical integration. The dhf-TZVP basis comprises relativistic effective core potentials (RECPs)[14] for Pb and I. The RI-J approximation was used throughout with universal Coulomb-fitting basis sets.[15] Geometries were optimized using the default convergence criteria (scfconv: 7, -energy 6, -gcart 3). None of the optimized equilibrium structures showed imaginary harmonic vibrational frequencies, and in all calculations, all of the occupied MOs had negative orbital energies.

To validate the preciseness of the chosen DFT approach, the cluster $[Nb_6I_8]^{2-}$ was calculated for comparison—and, as expected, resulted in 12 LMOs representing 2*c*2*e* single bonds along the edges of the Nb_6 octahedron.

Table 1. Crystallographic data of $[BMIm]_2[(Pb_6I_8)\{Mn(CO)_5\}_6]$

compound	$[BMIm]_2[(Pb_6I_8)\{Mn(CO)_5\}_6]$
sum formula	$Pb_6I_8\ Mn_6O_{30}N_4C_{46}H_{30}$
formula weight	3706.72 g mol^{-1}
crystal system/space group	triclinic/$P\bar{1}$
lattice parameters	
a	1325.8(3) pm
b	1350.1(3) pm
c	1352.2(3) pm
α	65.74(3)°
β	85.57(3)°
γ	67.07(3)°
V	2022.4(10) × 10^6 pm^3
formula units per cell, Z	1
density (calculated)	3.04 g cm^{-3}
absorption correction	numerical
absorption coefficient	16.46 mm^{-1}
measurement conditions	image plate diffractometer, Model IPDS II (STOE)
	λ(Mo Kα) = 71.073 pm, (*T* = 200 K)
measurement limits	$-18 \le h < 18$; $-16 \le k \le 18$; $0 \le l \le 18$, $2\theta_{max} = 59.5$
number of reflections	12829 (independent 8549)
refinement method	full-matrix least-squares on F^2
merging	R_{int} = 0.066
total number of least-squares parameters	453
largest diff. peak and hole	2.19/−3.72 e × 10^{-6} pm^3
figures of merit	
*R*1	0.047 (4411 $F_o > 4\sigma(F_o)$]
*R*1 (all data)	0.1158
*wR*2	0.0996
goodness of fit, GOF	0.722

RESULTS AND DISCUSSION

Ionic Liquid Mediated Synthesis. $[BMIm]_2[(Pb_6I_8)\{Mn(CO)_5\}_6]$ was prepared via ionic liquid mediated synthesis and obtained as bright red crystals. The title compound is highly sensitive to moisture and oxygen and—according to X-ray structure analysis based on single crystals—crystallizes triclinically in the space group $P\bar{1}$ (see Tables 1, 2). The crystals are very small and decompose slowly even at room temperature under release of CO. In addition to single-crystal structure analysis, the composition of the title compound was confirmed by energy-dispersive X-ray (EDX) analysis. Accordingly, the measured Mn:Pb:I ratio of 5.6:6:8.3 (scaled on Pb as the heaviest element) fits within the significance of the measurement with the calculated data (6:6:8).

The formation of $[BMIm]_2[(Pb_6I_8)\{Mn(CO)_5\}_6]$ can be rationalized based on the following reaction:

DOI: 10.1021/acs.inorgchem.5b00170
Inorg. Chem. 2015, 54, 3989−3994

Table 2. Selected Bond Distances of $[BMIm]_2[(Pb_6I_8)\{Mn(CO)_5\}_6]$, with $Mn_2(CO_{10})$ and PbI_2 as Reference Compounds

	Bond Distance (pm)		
bond	$[BMIm]_2[(Pb_6I_8)\{Mn(CO)_5\}_6]$	$Mn_2(CO_{10})$[a]	PbI_2[b]
Pb1−Mn1 (2×)	281.2(3)		
Pb2−Mn2 (2×)	279.9(3)		
Pb3−Mn3 (2×)	280.4(2)		
Pb1−I (I1−I4)	327.3(2)−335.1(2)		322.8
Pb2−I (I1−I4)	325.1(2)−334.9(2)		322.8
Pb3−I (I1−I4)	325.1(2)−332.6(2)		322.8
$Mn-C_{axial}$	179(2)−181(2)	181.1	
$Mn-C_{equatorial}$	183(2)−188(2)	185.0−186.5	
$C-O_{axial}$	114(2)−115(2)	113.4	
$C-O_{equatorial}$	109(2)−112(2)	112.4−113.1	

[a]Data taken from ref 24. [b]Data taken from ref 19.

$$6PbI_2 + 9Mn(CO)_5 \rightarrow [(Pb_6I_8)\{Mn(CO)_5\}_6]^{2-} + Mn^{2+} + 2MnI_2 + 15CO$$

The reaction is formally driven by the oxidation of manganese ($Mn^0 \rightarrow Mn^{2+}$) and the reduction of lead ($Pb^{2+} \rightarrow Pb^+$). Moreover, the entropic effect of releasing CO should not be underestimated. $[BMIm]_2[(Pb_6I_8)\{Mn(CO)_5\}_6]$ also decomposes slowly under CO release if a certain CO atmosphere and pressure are not available (such as that in a sealed glass ampule). Since the $[BMIm]^+$ cation of the ionic liquid is incorporated, the separation of $[BMIm]_2[(Pb_6I_8)\{Mn(CO)_5\}_6]$ from the ionic liquid is hampered by the more-or-less similar solubility of the ionic liquid and the title compound.

The ionic liquids can be considered to be essential for the preparation of $[BMIm]_2[\{PbMn(CO)_5\}_6I_8]$, in view of several aspects. On the one hand, ionic liquids are generally well-known for their excellent redox stability and their weakly coordinating properties. The option of performing reactions at mild temperature has been already validated as a unique feature of ionic liquids in inorganic synthesis.[16] Their potential for preparing new carbonyl clusters also has been reported.[17] These IL-specific properties can be regarded as a prerequisite for preparing $[BMIm]_2[\{PbMn(CO)_5\}_6I_8]$. The good solubility of all starting materials—but without significant coordination between the metal cations and the ionic liquid—are highly beneficial for obtaining Pb−Mn clusters such as $[\{PbMn(CO)_5\}_6I_8]^{2-}$, although, so far, considered less stable without any stabilization via alkyl or aryl ligands.[18]

Structural Characterization. $[BMIm]_2[\{PbMn(CO)_5\}_6I_8]$ is composed of $[(Pb_6I_8)\{Mn(CO)_5\}_6]^{2-}$ anions and $[BMIm]^+$ cations (see Figure 1). Central is a slightly distorted Pb_6 octahedron. This Pb_6 octahedron is surrounded by iodine, resulting in a Pb_6-centered, cubelike Pb_6I_8 unit. Furthermore, all vertices of the Pb_6 octahedron are linked to $Mn(CO)_5$ units. The Mn atoms can be considered to establish a Mn_6 superoctahedron that includes the I_8 cube and the central Pb_6 octahedron (Figure 1).

The central Pb_6 octahedron in $[(Pb_6I_8)\{Mn(CO)_5\}_6]^{2-}$ exhibits Pb−Pb distances ranging from 383.8(1) pm (Pb1−Pb3) to 394.0(1) pm (Pb1−Pb2) (see Figure 2). These values relate to twice the van-der-Waals radius (2 × 202 pm = 404 pm) and indicate the absence of any attractive Pb−Pb interaction. The Pb−Pb−Pb angles range from 88.4(1)° (∠Pb3−Pb2−Pb3) to 91.6(1)° (∠Pb2−Pb3−Pb2) and confirm a slight deviation of the ideal octahedron. Note that the central Pb_6 octahedron is nonfilled: cationic intercalation (e.g., H^+) can be excluded due to repulsion with the positively polarized Pb; anionic intercalation (e.g., C^{4-}, O^{2-}, I^-) can be excluded based on crystal structure analysis and the electroneutrality of the compound.

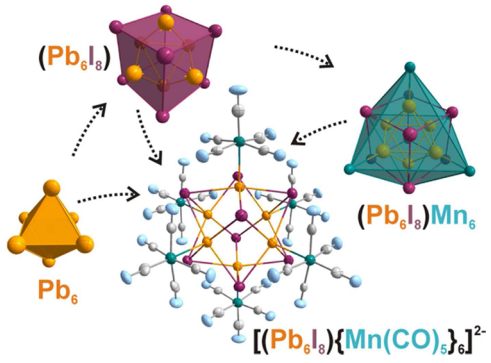

Figure 1. Scheme showing the $[(Pb_6I_8)\{Mn(CO)_5\}_6]^{2-}$ anion and the included different coordination polyhedra.

The cubelike (Pb_6I_8) unit exhibits Pb−I distances ranging from 325.1(2) pm (Pb3−I3) to 335.1(1) pm (Pb3−I2). These values range from almost similar to significantly elongated distances, in comparison to PbI_2 (323 pm) (see Table 2).[19] In view of the I−I−I angles ranging from 89.3(1) (∠I1−I2−I4) to 91.0(1)° (∠I1−I3−I4), the eight iodine atoms indeed form a slightly distorted cube. The I−Pb−I angles, finally, have values of 163.0(2) (∠I3−Pb2−I4) to 166.3(2)° (∠I2−Pb3−I3) and show that Pb is deflected out of the face of the I_8 cube (Figure 2). Again, this points to the absence of attractive Pb−Pb interactions.

The Pb−Mn distances in $[(Pb_6I_8)\{Mn(CO)_5\}_6]^{2-}$ range from 279.9(3) pm to 281.2(1) pm and clearly point to metal−metal bonding (see Table 2 and Figure 2). The Pb−Mn distances are elongated in comparison to known compounds with Pb−Mn bonds, such as $[\{Cp'(CO)_2Mn\}_2PbS^tBu]$ (257.4 pm, where Cp′ = $CH_3C_5H_4$)[20] or $[\{Cp'(CO)_2Mn\}Pb(SMes)_3]^-$ (261.7 pm, where Mes = mesityl).[21] This finding can be ascribed to steric hindrance due to the I atoms and the nearby carbonyl ligands (see Figures 1 and 2). In principle, Pb−Mn bonding is well-known for carbonyl clusters. The structural, magnetic, catalytic, and optical properties of such compounds have already been examined intensively.[18] Most often, isolated Pb−Mn, Mn−Pb−Mn, or Pb−Mn−Pb strings have been described.[18a] Larger Pb−Mn clusters are rare and limited to a planar $PbMn_3$ unit in $[(\eta^5\text{-}C_5H_4CH_3)Mn(CO)_2]_3Pb$.[22] Note that alkyl or aryl groups are essentially needed for all known Pb−Mn cluster compounds for electronical and/or sterical stabilization. In particular, halogenide-coordinated Pb−Mn clusters require such alkyl/aryl ligand stabilization, since halogenides have been reported to cause cleavage of the Pb−Mn bond.[18b,c] Hence, it is surprising that $[(Pb_6I_8)\{Mn(CO)_5\}_6]^{2-}$ is not stabilized by alkyl or aryl groups.

Altogether, the structure of the $[\{PbMn(CO)_5\}_6I_8]^{2-}$ cluster is obviously very similar to the well-known (M_6X_n) (n = 8−18) transition-metal cluster-type family. Among these transition-metal clusters, W_6Br_{12} (i.e., $[W_6Br_8]Br_{2/1}Br_{4/2}$, according to Niggli notation) might be the most obvious example (Figure 2b).[2] Another very similar structure is

DOI: 10.1021/acs.inorgchem.5b00170
Inorg. Chem. 2015, 54, 3989−3994

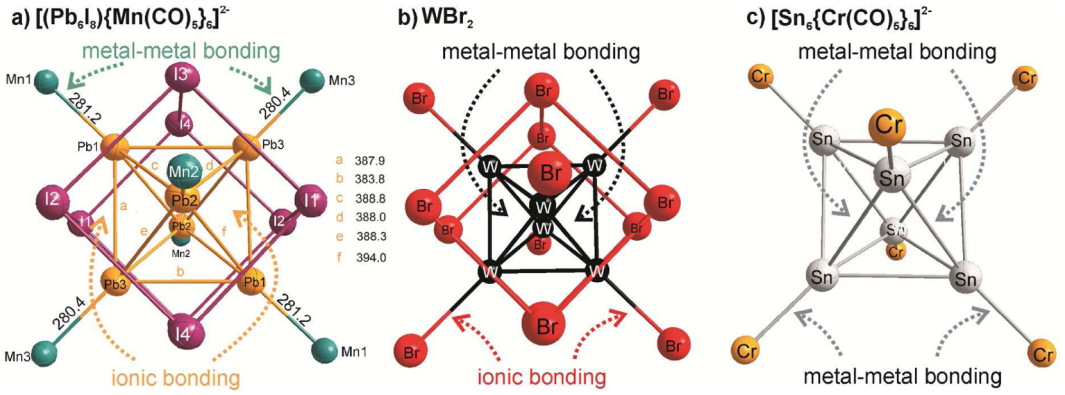

Figure 2. Comparison of cluster compounds with similar structure but different bonding situations: (a) $[(Pb_6I_8)\{Mn(CO)_5\}_6]^{2-}$ with selected distances (in pm); (b) W_6Br_{12} (i.e., $[W_6Br_8]Br_{2/1}Br_{4/2}$ according to Niggli notation),[2] and (c) the carbonyl cluster $[Sn_6\{Cr(CO)_5\}_6]^{2-}$.[7]

observed for the carbonyl cluster $[Sn_6\{Cr(CO_5)_6\}]^{2-}$ (Figure 2c).[7] Although structurally very similar, there is nevertheless a significant difference to the title compound. Whereas metal−metal interactions of the central W_6 and Sn_6 octahedra are essential for the bonding situation and existence in W_6Br_{12} and $[Sn_6\{Cr(CO_5)_6\}]^{2-}$, the central Pb_6 octahedron in $[\{PbMn(CO)_5\}_6I_8]^{2-}$ is without any Pb−Pb metal−metal bonding.

Bonding Situation. The bonding situation and oxidation state in $[BMIm]_2[(Pb_6I_8)\{Mn(CO)_5\}_6]$, first of all, can be estimated based on general concepts such as the isolobal principle or electronegativity considerations. Thus, the fragment $\{Mn(CO)_5\}^-$ is isolobal to I^-.[10] Taking the $\{Mn(CO)_5\}^-$ fragment as a pseudo-halogenide stresses the similarity between $[(Pb_6I_8)\{Mn(CO)_5\}_6]^{2-}$ and the transition-metal clusters $[M^{2+}{}_6X^-{}_8]X^-{}_2X^-{}_{4/2}$ (M = Mo, W; X = Cl, Br, I) even more (see Figure 2).[2,3] Electronegativity considerations (Pauling scale) indicate a higher electronegativity of lead (1.9), compared to manganese (1.5).[23] Thus, electron density of the Pb−Mn metal−metal bond is at least partly shifted to lead. Consequently, the oxidation state of lead results in Pb^0 and Mn^+.

In view of the CO ligands, two groups of Mn−C and C−O distances are observed (Table 2): CO ligands in *trans*-position to Pb atoms exhibit shorter Mn−C distances (ranging from 179(1) pm for Mn1−C5 to 181(1) pm for Mn3−C15) than CO ligands located *cis* to Pb (ranging from 183(2) pm for Mn1−C4 to 188(2) pm for Mn3−C14). In contrast, C−O distances of CO ligands *trans* to Pb are longer (ranging from 114(2) pm for C10−O10 to 115(2) pm for C5−O5) than of CO groups *cis* to Pb (ranging from 109(2) pm for C14−O14 to 112(2) pm for C9−O9). These findings are very comparable to dinuclear carbonyl metals, such as $Mn_2(CO)_{10}$.[24] This also suggests a similar bonding and charge distribution of manganese−thus, Mn^0 in $[BMIm]_2[(Pb_6I_8)\{Mn(CO)_5\}_6]$.

FT-IR spectra, first of all, show strong vibrations related to the $[BMIm]^+$ cation (ν(C−H): 3100−2800 cm^{-1}, fingerprint area: 1500−500 cm^{-1}) as well as CO-related vibrations (ν(C≡O): 2100−1900 cm^{-1}) (Figure 3). In view of the crystallographically different CO groups in $[(Pb_6I_8)\{Mn(CO)_5\}_6]^{2-}$, five different CO vibrations (2063, 2008, 1980, 1964, 1953 cm^{-1}) can be differentiated by FT-IR spectroscopy (see Figure 3 and Table 1). Since the six $Mn(CO)_5$ groups are not symmetry equivalent due to the lower space-group symmetry in comparison to the site symmetry of the $[(Pb_6I_8)\{Mn(CO)_5\}_6]^{2-}$ cluster anion various CO vibrations are visible that are partly overlapping. Altogether, these IR data are again

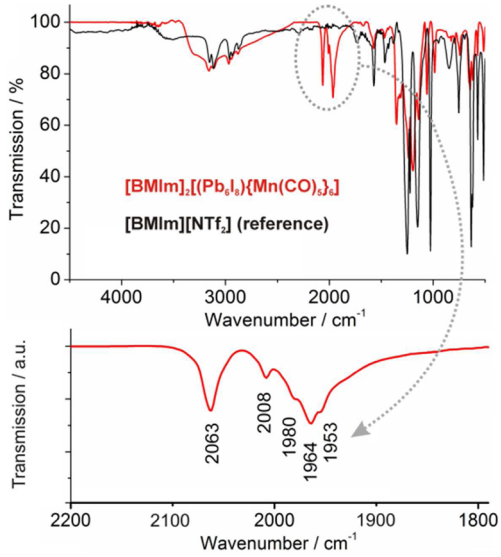

Figure 3. FT-IR spectrum of $[BMIm]_2[(Pb_6I_8)\{Mn(CO)_5\}_6]$ (ionic liquid $[BMIm](NTf_2]$ shown as a reference).

very comparable to $Mn_2(CO)_{10}$,[25] and point to a similar bonding situation and zerovalent manganese in the title compound.

To verify the bonding situation of Pb and Mn in $[(Pb_6I_8)\{Mn(CO)_5\}_6]^{2-}$, DFT calculations were performed with the TURBOMOLE program at the TPSS/dhf-TZVP level.[26] To this concern, a Pipek−Mezey localization procedure resulted in six 2*c*2*e* single bonds for Pb−Mn and one *s*-type orbital at each Pb atom, giving a oxidation state of +1 (Pb^+; see Figure 4). The remaining localized molecular orbitals (LMOs)

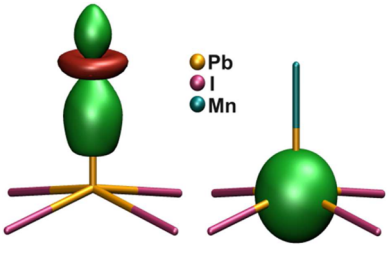

Figure 4. Pipek−-Mezey localized molecular orbitals representing the Pb−Mn bond (left) and the 6*s*-orbital of Pb (right) in $[(Pb_6I_8)\{Mn(CO)_5\}_6]^{2-}$ (isosurfaces of the amplitude plotted at $\pm 0.1 a_0^{-3/2}$).

DOI: 10.1021/acs.inorgchem.5b00170
Inorg. Chem. 2015, 54, 3989−3994

of the valence shell are localized at the I atoms (four LMOs per I atom) or within the $Mn(CO)_5$ units (28 LMOs per $Mn(CO)_5$ unit). These findings suggest oxidation states of Pb^{+I} and Mn^0. Notably, no LMOs are present between the Pb atoms of the central Pb_6 octahedron. This clearly indicates a nonfilled Pb_6 octahedron and the absence of attractive Pb−Pb interactions as it has been already suggested by the Pb−Pb distances, the deflection of the Pb atoms to the outside of the I_8 cube, and electronegativity considerations.

Mulliken population analysis and natural population analysis (NPA)[27] of $[(Pb_6I_8)\{Mn(CO)_5\}_6]^{2-}$ and various DFT-calculated reference compounds such as the formal cluster fragment $[PbMn(CO)_5]^+$, the formal cluster monomer $[PbMn(CO)_5]I$, or selected DFT-calculated compounds such as $[(CO)_5Mn-PbX_3]$ and $(CO)_5Mn-PbX_2-Mn(CO)_5$ (X = Cl, Br, I; methyl (Me), ethyl (Et), phenyl (Ph)) consistently indicate a significantly lower cationic charge on lead for $[(Pb_6I_8)\{Mn(CO)_5\}_6]^{2-}$ (Mulliken: +0.50, NPA: +0.58) than for the DFT-calculated reference compounds (see Table 3).

Table 3. Mulliken and NPA Population Analysis of $[(Pb_6I_8)\{Mn(CO)_5\}_6]^{2-}$ and Various DFT-Calculated Reference Compounds

	Mulliken		NPA	
compound	Pb	Mn	Pb	Mn
$[(Pb_6I_8)\{Mn(CO)_5\}_6]^{2-}$	+0.50	−0.47	+0.58	−1.10
$[PbMn(CO)_5]^+$ fragment	+1.05	−0.46	+1.23	−1.18
$[PbMn(CO)_5]I$ monomer	+0.64	−0.46	+0.77	−1.14
$(CO)_5Mn-PbCl_3$	+0.91	−0.66	+1.15	−1.10
$(CO)_5Mn-PbBr_3$	+0.80	−0.63	+0.93	−1.09
$(CO)_5Mn-PbI_3$	+0.65	−0.60	+0.62	−1.08
$(CO)_5Mn-PbMe_3$	+0.83	−0.50	+1.10	−1.11
$(CO)_5Mn-PbEt_3$	+0.76	−0.49	+1.10	−1.10
$(CO)_5Mn-PbPh_3$	+0.77	−0.55	+1.20	−1.10
$(CO)_5Mn-PbIEt_2$	+0.66	−0.50	+0.99	−1.10
$[(CO)_5Mn-PbI_2]^-$	+0.51	−0.36	+0.59	−1.06
$[(CO)_5Mn-PbI_4]^-$	+0.62	−0.48	+0.63	−1.06
$(CO)_5Mn-PbCl_2-Mn(CO)_5$	+0.78	−0.54	+0.89	−1.08
$(CO)_5Mn-PbBr_2-Mn(CO)_5$	+0.75	−0.53	+0.75	−1.08
$(CO)_5Mn-PbI_2-Mn(CO)_5$	+0.63	−0.50	+0.54	−1.07
$(CO)_5Mn-PbMe_2-Mn(CO)_5$	+0.71	−0.47	+0.86	−1.08
$(CO)_5Mn-PbEt_2-Mn(CO)_5$	+0.70	−0.46	+0.90	−1.08
$(CO)_5Mn-PbPh_2-Mn(CO)_5$	+0.78	−0.50	+0.96	−1.08

Moreover, although the charge on lead is significantly affected by the neighboring atoms (Mulliken: +0.50 to +1.05, NPA: +0.54 to +1.23), the negative charge on manganese remains almost unchanged (Mulliken: −0.63 to −0.36, NPA: −1.18 to −1.06). These findings indicate that significantly more electron density is shifted from iodine to lead for $[(Pb_6I_8)\{Mn(CO)_5\}_6]^{2-}$ than in the DFT-calculated reference compounds (Table 3). In contrast, the charge on manganese is almost independent from lead and iodine. In summary, Mulliken and NPA population analyses confirm a comparably high electron density on lead, especially in comparison to typical Pb^{2+}-containing compounds.

Based on DFT calculations, finally, the Pb−Mn distance in $[(Pb_6I_8)\{Mn(CO)_5\}_6]^{2-}$ can be compared with various DFT-calculated reference compounds (Table 4). The calculated value of 294.4 pm is much longer than in all DFT-calculated references, except for the compound $[(CO)_5Mn-PbI_2]^-$ (307.5 pm). The Mulliken and NPA charges of $[(CO)_5Mn-PbI_2]^-$ agree as well with those on the title compound, indicating a comparable bonding situation and oxidation states Pb^+ and Mn^0. Concerning the Pb−Mn distances, the enormous difference between $[(Pb_6I_8)\{Mn(CO)_5\}_6]^{2-}$ (294.4 pm) and the geometry-optimized $[PbMn(CO)_5]^+$ fragment (261.7 pm) is particularly remarkable (see Table 4). This finding indicates that the Pb−Mn distance, in principle, could be very short and again points to the steric effect related to the adjacency of iodine and oxygen (from the carbonyl groups) for $[(Pb_6I_8)\{Mn(CO)_5\}_6]^{2-}$. Based on the DFT-calculated reference compounds, again, the steric repulsion and the elongated Pb−Mn bond are confirmed.

Table 4. Pb−Mn Distance in $[(Pb_6I_8)\{Mn(CO)_5\}_6]^{2-}$ and Comparison to DFT-Calculated Reference Compounds

compound	Pb−Mn bond distance (pm)
$[(Pb_6I_8)\{Mn(CO)_5\}_6]^{2-}$	294.4
$[(PbMn(CO)_5]^+$ fragment	261.7
$[PbMn(CO)_5]I$ monomer	283.9
$(CO)_5Mn-PbCl_3$	272.2
$(CO)_5Mn-PbBr_3$	274.4
$(CO)_5Mn-PbI_3$	275.7
$(CO)_5Mn-PbMe_3$	280.9
$(CO)_5Mn-PbEt_3$	283. 7
$(CO)_5Mn-PbPh_3$	281.8
$(CO)_5Mn-PbIEt_2$	279.3
$[(CO)_5Mn-PbI_2]^-$	307.5
$[(CO)_5Mn-PbI_4]^-$	283.0
$(CO)_5Mn-PbCl_2-Mn(CO)_5$	277.0, 278.8
$(CO)_5Mn-PbBr_2-Mn(CO)_5$	278.1, 279.6
$(CO)_5Mn-PbI_2-Mn(CO)_5$	281.7, 281.7
$(CO)_5Mn-PbMe_2-Mn(CO)_5$	287.3
$(CO)_5Mn-PbEt_2-Mn(CO)_5$	285.8
$(CO)_5Mn-PbPh_2-Mn(CO)_5$	284.7

CONCLUSION

$[BMIm]_2[(Pb_6I_8)\{Mn(CO)_5\}_6]$ is unique in view of different aspects. $[(Pb_6I_8)\{Mn(CO)_5\}_6]^{2-}$ is not established by metal−metal interactions of the central Pb_6 octahedron but predominantly by ionic Pb−I interactions with the surrounding I_8 shell. The latter is contrary to the topologically similar and well-known (M_6X_n) (n = 8−18) transition-metal halogenide and transition-metal chalcogenide clusters. Based on the isolobal principle, electronegativity considerations, and bond lengths, as well as DFT calculations including Mulliken and NPA population analyses, in summary, the charge distribution of lead and manganese is best adopted by Pb^+ and Mn^0. In contrast to known Pb−Mn clusters, no alkyl or aryl ligands are needed for electronic and/or steric stabilization of the title compound. Altogether, $[(Pb_6I_8)\{Mn(CO)_5\}_6]^{2-}$ is topologically very similar to the well-known octahedral (M_6X_n) transition-metal clusters such as those observed in W_6Br_{12} (i.e., $[W_6Br_8]Br_{2/1}Br_{4/2}$, according to Niggli notation, or carbonyl clusters, such as $[Sn_6\{Cr(CO_5)_6\}]^{2-}$). Despite the similar structures, however, $[(Pb_6I_8)\{Mn(CO)_5\}_6]^{2-}$ exhibits an unprecedented inverted bonding situation: The cluster anion does not exhibit any metal−metal bonding of the central Pb_6 octahedron, but Pb−Mn metal-to-metal interactions are directed to the outside of the Pb_6 octahedron.

DOI: 10.1021/acs.inorgchem.5b00170
Inorg. Chem. 2015, 54, 3989−3994

AUTHOR INFORMATION

Corresponding Author

*E-mail: claus.feldmann@kit.edu.

Notes

The authors declare no competing financial interest.

ACKNOWLEDGMENTS

S.W. and C.F. acknowledge the Priority Programme SPP 1708, "Material Synthesis near Room Temperature", of the Deutsche Forschungsgemeinschaft (DFG) for funding. Furthermore, the authors are grateful to the DFG for the funding of analytical equipment.

REFERENCES

(1) (a) Braunstein, P., Oro, L. A., Raithby, P. R., Eds. *Metal Clusters in Chemistry*; Wiley−VCH: Weinheim, Germany, 2008. (b) Corbett, J. D. *J. Solid State Chem.* **1981**, *37*, 335. (Review) (c) Simon, A. *Angew. Chem., Int. Ed.* **1988**, *27*, 159 (Review).

(2) (a) Schäfer, H.; von Schnering, H.-G.; Tillack, J. V.; Kuhnen, F.; Woehrle, H.; Baumann, H. *Z. Anorg. Allg. Chem.* **1967**, *353*, 281. (b) Siepmann, R.; von Schnering, H.-G.; Schäfer, H. *Angew. Chem., Int. Ed.* **1967**, *6*, 637. (c) Franolic, J. D.; Long, J. R.; Holm, R. H. *J. Am. Chem. Soc.* **1995**, *117*, 8139.

(3) (a) Simon, A.; von Schnering, H.-G.; Schäfer, H. *Z. Anorg. Allg. Chem.* **1967**, *353*, 295. (b) Artelt, H. M.; Meyer, G. *Z. Kristallogr.* **1993**, *206*, 306. (c) Corbett, J. D.; Daake, R. L.; Poeppelmeier, K. R.; Guthrie, D. H. *J. Am. Chem. Soc.* **1978**, *100*, 652.

(4) Köhler, J.; Tischtau, R.; Simon, A. *J. Chem. Soc., Dalton Trans.* **1991**, 829.

(5) (a) Chevrel, R.; Hirrien, M.; Sergent, M. *Polyhedron* **1986**, *5*, 87.

(6) Kertesz, M.; Hoffmann, R. *J. Am. Chem. Soc.* **1984**, *106*, 3453.

(7) Schiemenz, B.; Huttner, B. *Angew. Chem., Int. Ed.* **1993**, *32*, 297.

(8) von Schnering, H.-G. *Angew. Chem., Int. Ed. Engl.* **1981**, *20*, 33 (Review).

(9) (a) Wang, B.; Molina, L. M.; López, M. J.; Rubio, A.; Alonso, J. A.; Stott, M. J. *Ann. Phys.* **1998**, *7*, 107. (b) Li, X. P.; Lu, W.-C.; Zang, Q.-J.; Chen, G.-J.; Wang, C. Z.; Ho, K. M. *J. Phys. Chem. A* **2009**, *113*, 6217. (c) Baldes, A.; Gulde, R.; Weigend, F. *J. Clust. Sci.* **2011**, *22*, 355.

(10) Hoffmann, R. *Angew. Chem., Int. Ed. Engl.* **1982**, *21*, 711.

(11) *TURBOMOLE V6.5, 2013*, A development of the University of Karlsruhe and the Forschungszentrum Karlsruhe GmbH, 1989−2007, TURBOMOLE GmbH, since 2007; available from http://www.turbomole.com.

(12) Tao, J.; Perdew, J. P.; Staroverov, V. N.; Scuseria, G. E. *Phys. Rev. Lett.* **2003**, *91*, 146401.

(13) Weigend, F.; Baldes, A. *J. Chem. Phys.* **2010**, *133*, 174102.

(14) (a) Metz, B.; Stoll, H.; Dolg, M. *J. Chem. Phys.* **2000**, *113*, 2563. (b) Peterson, K. A.; Shepler, B. C.; Figgen, D.; Stoll, H. *J. Phys. Chem. A* **2006**, *110*, 13877.

(15) Weigend, F. *Phys. Chem. Chem. Phys.* **2006**, *8*, 1057.

(16) (a) Wasserscheid, P.; Welton, P. *Ionic Liquids in Synthesis*; Wiley−VCH: Weinheim, Germany, 2008. (b) Freudenmann, D.; Wolf, S.; Wolff, M.; Feldmann, C. *Angew. Chem., Int. Ed.* **2011**, *50*, 11050 (Review). (c) Ahmed, E.; Ruck, M. *Dalton Trans.* **2011**, *40*, 9347 (Review).

(17) (a) Dyson, P. J. *Transition Met. Chem.* **2002**, *27*, 353 (Review). (b) Wolf, S.; Winter, F.; Pöttgen, R.; Middendorf, N.; Klopper, W.; Feldmann, C. *Chem.—Eur. J.* **2012**, *18*, 13600. (c) Oelkers, B.; Venker, A.; Sundermeyer, J. *Inorg. Chem.* **2012**, *51*, 4636.

(18) (a) Leong, V. S.; Copper, N. J. *Organometallics* **1988**, *7*, 2080. (b) Haupt, H. J.; Schubert, W.; Huber, F. *J. Organomet. Chem.* **1973**, *54*, 231. (c) Booth, M. R.; Cardin, D. J.; Carey, N. A. D.; Clark, H. C.; Sreenathan, B. R. *J. Organomet. Chem.* **1970**, *21*, 171.

(19) Minagawa, T. *Acta Crystallogr., Sect. A: Cryst. Phys. Diffr., Theor. Gen. Crystallogr.* **1975**, *A31*, 823.

(20) Ettel, F.; Huttner, G.; Zsolnai, L. *Angew. Chem.* **1989**, *10*, 1525.

(21) (a) Ettel, F.; Schollenberger, M.; Schiemenz, B.; Imhof, W.; Huttner, G.; Zsolnai, L. *J. Organomet. Chem.* **1994**, *476*, 207. (b) Ettel, F.; Schollenberger, M.; Schiemenz, B.; Huttner, G.; Zsolnai, L. *J. Organomet. Chem.* **1994**, *476*, 153.

(22) Kneuper, H.-J.; Herdtweck, E.; Herrmann, W. A. *J. Am. Chem. Soc.* **1987**, *109*, 2508.

(23) (a) Allred, A. L. *J. Inorg. Nucl. Chem.* **1961**, *17*, 215. (b) Jansen, M.; Wedig, U. *Angew. Chem., Int. Ed.* **2008**, *47*, 10026.

(24) (a) Dahl, L. F.; Rundle, R. E. *Acta Crystallogr.* **1963**, *16*, 419. (b) Churchill, M. R.; Amoh, K. N.; Wasserman, H. J. *Inorg. Chem.* **1981**, *20*, 1609.

(25) Haas, H.; Sheline, R. K. *J. Chem. Phys.* **1967**, *47*, 2996.

(26) (a) Pipek, J.; Mezey, P. G. *J. Chem. Phys.* **1989**, *90*, 4916. (b) Weigend, F.; Baldes, A. *J. Chem. Phys.* **2010**, *133*, 174102. (c) Tao, J.; Perdew, J. P.; Staroverov, V. N.; Scuseria, G. E. *Phys. Rev. Lett.* **2003**, *91*, 146401. (d) Furche, F.; Ahlrichs, R.; Hättig, C.; Klopper, W.; Sierka, M.; Weigend, F. *WIREs Comput. Mol. Sci.* **2014**, *4*, 91.

(27) (a) Mulliken, R. S. *J. Chem. Phys.* **1955**, *23*, 1833. (b) Reed, A. E.; Weinstock, R. B.; Weinhold, F. *J. Chem. Phys.* **1985**, *83*, 735.

DOI: 10.1021/acs.inorgchem.5b00170
Inorg. Chem. 2015, 54, 3989−3994